

Original Research Article

Pattern and distribution of lung parenchymal changes in COVID-19 infection on high resolution computed tomography: a descriptive cross-sectional study

Joe Jose*, Kiran V. Kalenahalli, Sravanthi Yerram, Rishikesh M. Itagi, Sowmya Eswara

Department of Radiology, Sagar Hospitals, Tilak Nagar, Jayanagar, Bengaluru, Karnataka, India

Received: 20 September 2022

Revised: 31 October 2022

Accepted: 07 November 2022

*Correspondence:

Dr. Joe Jose,

E-mail: joejoseminu@gmail.com

Copyright: © the author(s), publisher and licensee Medip Academy. This is an open-access article distributed under the terms of the Creative Commons Attribution Non-Commercial License, which permits unrestricted non-commercial use, distribution, and reproduction in any medium, provided the original work is properly cited.

ABSTRACT

Background: This was a descriptive cross-sectional study conducted in a tertiary care hospital in south India during the peak of the COVID-19 infection pandemic in India between June 2020 to June 2021. HRCT lung parenchymal findings of patients with COVID-19 infection were studied, and the pattern and distribution of various lung parenchymal changes in each lung were described. HRCT lung findings were further correlated with clinical findings and clinical severity, which further helped in the clinical management of patients.

Methods: This descriptive cross-sectional study was done at Sagar Hospitals, Tilak Nagar, Jayanagar, Bengaluru on a total of 111 RT-PCR positive COVID-19 patients in the age group 18 to 80. HRCT lung imaging findings were studied from June 2020 to June 2021 during the pandemic. These findings were further correlated with clinical findings and the clinical severity of the patient.

Results: This study showed that chest CT findings in COVID-19 infection are variable. Ground glass opacity was the most common lesion observed, followed by Air space opacification and consolidation with an air bronchogram. In some cases, a crazy-paving pattern, subpleural linear bands, subpleural reticulations and fibrotic streaks were observed. A few cases showed traction bronchiectasis due to adjacent lung fibrosis and lung cyst within lesions. The lesion distribution was both bilateral (more common) and unilateral and showed peripheral predominance. There was a positive correlation between the CT severity score and clinical grading and the clinical severity of the patient.

Conclusions: HRCT lung findings in COVID-19 patients were described in detail, including predominant lesion, predominant pattern, distribution in detail with reference to each lung segment, laterality, and correlation with clinical severity.

Keywords: COVID-19, High resolution computed tomography, HRCT, GGO, Ground glass opacities, Pneumonia

INTRODUCTION

This study was conducted in a hospital in Bengaluru, South India, during the peak of the COVID-19 infection pandemic in India. COVID-19 is a respiratory virus with a predominant clinical presentation with respiratory symptoms. HRCT is the investigation of choice in most lung infections. As it is a new virus with no literature on clinical or imaging findings, this study carries the

importance of describing the various HRCT chest findings in COVID-19 infection in Indian ethnicity.

Several international studies have described many typical findings in HRCT lung in Covid patients.¹⁻³ Various studies described the most common finding in COVID-19 as peripheral predominant ground-glass opacities.⁴⁻⁷ The extent and severity of these lesions have a significant impact on prognosis.⁸

Few studies have quantified lung involvement of Covid infection on CT. Quantitative measurement of lung involvement in COVID-19 pneumonia can help clinicians determine the severity of the case.⁹ Some studies have described that the patient's clinical symptoms may be directly related to the CT severity score, and CT may help predict the patient's clinical recovery or disease progression.¹⁰

As COVID-19 has evolved as a global pandemic, the aim of this study was to identify distinct lung abnormalities on HRCT chest in COVID-19 infection, focusing on the pattern and distribution of lung findings in high-resolution CT and identify any association between clinical severity and CT severity of covid patients in the local population.

METHODS

We did the study from June 2020 to June 2021 at Sagar Hospitals, Tilak Nagar, Jayanagar, Bengaluru after ethical committee approval. Our sample size was 111.

Inclusion criteria

COVID-19 RT-PCR positive patients in the age group 18 to 80 referred to the department of radiology for HRCT chest were included in the study.

Exclusion criteria

COVID-19 RT-PCR positive patients with medical records and clinical history of pre-existing lung pathologies like pulmonary tuberculosis, lung malignancies, interstitial lung disease, bronchiectasis, metastases etc., were excluded from the study. COVID-19 RT-PCR positive patients with pleural effusion were excluded from the study to avoid bias of lung congestion in pleural effusion. HRCT with extensive movement blur due to patients' inability to hold breath were excluded from the study due to poor image quality.

Single time point CT study of each patient at the first visit to the radiology department was reviewed, and follow-up scans were not included in this study. Patients' demographic, clinical, treatment details and outcome measures were obtained from the medical records.

Computed tomography was performed on a multi-row detector CT scanner using HIGH-RESOLUTION CT protocol in full inspiration breath-hold without contrast. Thin sections of slice thickness 0.625 mm were acquired and post-processed in a high-spatial-frequency reconstruction algorithm using isotropic multi-planar reconstructions on an advanced workstation.

HRCT images were reviewed by two qualified radiologists. Clinical data regarding severity grading of RT-PCR positive patients were reviewed from medical

records. Various patterns and distribution of lung parenchymal findings were documented.

Clinical grading was done as below:

The patient's medical history was reviewed from the hospital records. Clinical severity was graded as mild, moderate, severe and critical disease.^{8,11,12} Patients who were asymptomatic or mildly symptomatic (with fatigue and fever) were classified as a mild disease. The moderate disease group included cough with evidence of lower respiratory disease during clinical assessment and oxygen saturation (SpO₂) ≥94% on room air. Severe disease included respiratory distress, respiratory rate ≥30 beats per minute, SpO₂ ≤93% at resting and arterial PaO₂/FiO₂ ≤300 mmHg. Critical diseases included respiratory failure, need for mechanical ventilation, shock combined with other organ failures, and requiring intensive care.

HRCT lung parenchymal findings were reviewed as below:^{3,13-15}

Types of lung lesions

Focal areas of a slight increase in lung attenuation without obscuring underlying vascular structures were classified as ground glass haziness (GGH). Small (≤4 cm) round areas of increased lung attenuation/consolidation obscuring underlying lung vessels and airways were classified as air space opacification (ASO). Sizeable focal areas (>4 cm) of frank consolidation with air bronchogram were classified as consolidation with air bronchogram (CON), and mixed pattern opacities included mixed (Mixed) types of lesions.

Number of lung lesions

Less than or equal to five lesions in each lung segment were considered as few (FEW), while more than five lesions were considered as multiple (MUL).

Predominant pattern of lung lesions

Predominant pattern of lesions in each segment of the lung was described by noting the most commonly occurring distribution pattern in all the segments. More than 70% of the pattern in a segment is defined as either predominant ground-glass haziness pattern (PGGH), predominant Air space opacification pattern (PASO) or predominant consolidation with air bronchogram pattern (PCON). A mixed pattern was defined as a mixed type of opacities in a segment without any predominant pattern of lesions (MIX).

Additional lung findings

Subpleural linear bands (SPB) are seen as a thin 1-3 mm thick linear shadow within 1 cm from the pleural surface. Crazy paving pattern (CPP) is defined as thickened

interlobular septa and intralobular septal lines with superimposed ground-glass opacities. Subpleural reticulations and fibrotic streaks (SRFB) are irregular subpleural reticulations and fibrotic changes without honeycombing. Traction bronchiectasis (TB) is a subtype of bronchiectasis in which the bronchi are dilated due to mechanical traction from the fibrosis of adjacent lung parenchyma. Lung cyst/air bubbles (vacuolar sign) within lung opacity (LC) are small air-containing spaces within the ground-glass opacity, less than 5 mm in size.

Predominant distribution of lung lesions

Predominant distribution pattern of lesions in each segment was described as peripheral distribution pattern (PP) if more than 70% of lesions in peripheral 1/3rd of segments, central distribution pattern (CP) if more than 70% of lesions in the inner 2/3rd of segments and mixed distribution pattern (MP) when there is diffuse distribution pattern in segments without peripheral or central predominance.

Location of lung lesions

Lesion occurrence in each bronchopulmonary segment of the lung was described. Bronchopulmonary segments of the right lung included apical, anterior and posterior segments of the upper lobe; medial, lateral segments of the middle lobe and superior, anterior, posterior, medial and lateral segments of the lower lobe and bronchopulmonary segments of the left lung included apical, anterior and posterior segments of upper lobe; superior and inferior segments of lingular segment and superior, anterior, posterior, medial and lateral segments of the lower lobe.

CT Grading of lung involvement¹⁶⁻¹⁸

The involvement in each 20 segment regions was scored 0 to 2. A score of 0 was assigned if there were no opacities, a score of 1 for opacities involving less than 50% of the lung segment and a score of 2 for opacities involving more than 50% of the lung segment. Scores in each 20-segment region were added, and the total lung involvement was graded as normal, mild, moderate, and severe. CT was graded as normal if the score was 0, mild if the score was 1 to 10, moderate if the score was 11 to 19, and severe if the score was 20 to 40.

The acquired data was entered into a Microsoft Excel datasheet and analysed using SPSS version 23 (statistical package for the social sciences) software. Demographic and categorical data were expressed as frequencies and percentages. Continuous data were expressed as mean ± standard deviation (SD). Fisher exact test was used to find the significant association between clinical severity and CT severity of patients. Spearman’s rank correlation was used to find the strength of the correlation between

CT severity and clinical severity. P value <0.05 was considered statistically significant.

RESULTS

This study included a total of 111 RT-PCR-positive Covid-19 patients. The mean age±SD (range) was 52.37±13.38 (22-79), and M:F was 78:33. Most of the patients were non-ICU cases; some were ICU admitted, and a few were on ventilatory support. The data obtained from HRCT lung and the clinical details are tabulated as below:

Table 1: Demographics, baseline clinical characteristics and HRCT lung findings of the cohort.

Variable (n=111)	N (%)
Age (mean±SD)	52.37±13.38
M:F	78:33
Clinical severity	
Mild	-
Moderate	-
Severe	-
Critical	-
Primary type of lesions n (%)	
GGH	94 (84.6)
ASO	78 (70.2)
CON	37 (33.3)
Predominant pattern type n (%)	
PGGH	58 (52.2)
PASO	27 (24.3)
PCON	5 (4.5)
Mixed pattern	9 (8.1)
NIL	12 (10.8)
Additional findings n (%)	
CPP	21 (18.9)
SPB	24 (21.6)
SRFB	11 (9.9)
TB	9 (8.1)
LC	2 (1.8)
Predominant distribution n (%)	
PP	76 (68.4)
CP	5 (4.5)
MP	18 (16.2)
NIL	12 (10.8)
Laterality n (%)	
Bilateral lesions	93 (93.9)
Unilateral lesions	6 (6.1)
Right lung (5)	
Right upper lobe only	1
Right upper and lower lobes	1
Right lower lobe only	3
Left lung (1)	
Left upper and lower lobes	1

Table 2: Predominant pattern and distribution of lung lesion in each segment.

Predominant pattern n (%)										
	Right upper lobe segments			Right middle lobe segments		Right lower lobe				
	Apical	Anterior	Posterior	Medial	Lateral	Superior	Posterior	Anterior	Medial	Lateral
PGGH	42 (60.87)	55 (67.90)	57 (67.86)	52 (70.27)	56 (70)	44 (48.89)	39 (48.15)	41 (54.67)	38 (51.35)	44 (56.41)
PASO	18 (26.09)	17 (20.99)	17 (20.24)	15 (20.27)	19 (23.75)	30 (33.33)	28 (34.57)	24 (32.00)	26 (35.14)	27 (34.62)
PCON	2 (2.90)	2 (2.47)	3 (3.57)	2 (2.70)	0 (0)	8 (8.89)	5 (6.17)	3 (4)	2 (2.70)	0 (0)
MIX	7 (10.14)	7 (8.64)	7 (8.33)	5 (6.76)	5 (6.25)	8 (8.89)	9 (11.11)	7 (9.33)	8 (10.81)	7 (8.97)
	Left upper lobe segments					Left lower lobe segments				
	Apical	Anterior	Posterior	Superior lingular	Inferior lingular	Superior	Posterior	Anterior	Medial	Lateral
PGGH	45 (69.23)	55 (70.51)	56 (70.89)	42 (56)	43 (56.58)	41 (48.24)	42 (52.50)	39 (53.42)	37 (55.22)	44 (59.46)
PASO	14 (21.54)	15 (19.23)	15 (18.99)	24 (32%)	24 (31.58)	32 (37.65)	28 (35.00)	23 (31.51)	21 (31.34)	20 (27.03)
PCON	0 (0)	1 (1.28)	1 (1.27)	2 (2.67)	1 (1.32)	4 (4.71)	3 (3.75)	3 (4.11)	1 (1.49)	1 (1.35)
MIX	6 (9.23)	7 (8.97)	7 (8.86)	7 (9.33)	8 (10.53)	8 (9.41)	7 (8.75)	8 (10.96)	8 (11.94)	9 (12.16)
Additional findings in each segment n (%)										
	Right upper lobe segments			Right middle lobe		Right lower lobe segments				
	Apical	Anterior	Posterior	Medial	Lateral	Superior	Posterior	Anterior	Medial	Lateral
CPP	7 (6.31)	12 (10.81)	14 (12.61)	5 (4.50)	3 (2.70)	3 (2.70)	2 (1.80)	1 (0.90)	1 (0.90)	2 (1.80)
SPB	--	--	5 (4.50)	1 (0.90)	1 (0.90)	9 (8.11)	14 (12.61)	12 (10.81)	13 (11.71)	8 (7.21)
TB	--	--	1 (0.90)	--	--	--	3 (2.70)	4 (3.60)	3 (2.70)	--
LC	--	--	--	--	--	--	1 (0.90)	--	--	--
SRFB	--	--	--	--	--	--	6 (5.41)	7 (6.31)	8 (7.21)	1 (0.90)
	Left upper lobe segment					Left lower lobe segment				
	Apical	Anterior	posterior	Superior lingular	Inferior lingular	Superior	Posterior	Anterior	Medial	Lateral
CPP	8 (7.21)	11 (9.91)	12 (10.81)	8 (7.21)	4 (3.60)	3 (2.70)	1 (0.90)	--	1 (0.90)	1 (0.90)
SPB	--	1 (0.90)	1 (0.90)	5 (4.50)	4 (3.60)	5 (4.50)	14 (12.61)	10 (9.01)	10 (9.01)	11 (9.91)
SRFB	--	--	--	--	--	--	3 (2.70)	2 (1.80)	5 (4.50)	2 (1.80)
TB	--	--	--	--	--	--	1 (0.90)	--	--	--
LC	--	--	--	--	--	--	1 (0.90)	--	--	--
Predominant distribution n (%)										
	Right upper lobe segments			Right middle lobe segments		Right lower lobe segments				
	Apical	Anterior	Posterior	Medial	Lateral	Superior	Posterior	Anterior	Medial	Lateral
CP	5 (7.25)	6 (7.41)	3 (3.61)	9 (12.16)	3 (3.75)	5 (5.56)	1 (1.23)	3 (3.95)	1 (1.35)	0 (0)
MP	23 (33.33)	21 (25.93)	20 (24.10)	32 (43.24)	21 (26.25)	30 (33.33)	15 (18.25)	15 (19.74)	14 (18.92)	15 (19.23)
PP	41 (59.42)	54 (66.67)	60 (72.29)	33 (44.59)	56 (70)	55 (61.11)	65 (80.25)	58 (76.32)	59 (79.73)	63 (80.77)
	Left upper lobe segments					Left lower lobe segments				
	Apical	Anterior	Posterior	Superior lingular	Inferior lingular	Superior	Posterior	Anterior	Medial	Lateral
CP	2 (3.13)	3 (3.85)	2 (2.63)	4 (5.33)	2 (2.63)	5 (5.88)	0 (0)	1 (1.37)	0 (0)	0 (0)
MP	26 (40.63)	26 (33.33)	22 (28.95)	24 (32)	22 (28.95)	33 (38.82)	16 (20.25)	17 (23.29)	14 (20.90)	15 (20.27)
PP	36 (56.25)	49 (62.82)	52 (68.42)	47 (62.67)	52 (68.42)	47 (55.29)	63 (79.75)	55 (75.34)	53 (79.10)	59 (79.73)

Table 3: Association between CT severity and clinical severity of patients.

		CT severity				Total n (%)	P value*
		Normal	Mild	Moderate	Severe		
Clinical severity	Mild	12	0	0	0	12 (10.8)	<0.001
	Moderate	0	9	45	10	64 (57.6)	
	Severe	0	0	1	23	24 (21.6)	
	Critical	0	0	0	11	11 (9.9)	
Total n (%)		12 (10.8)	9 (8.1)	46 (41.4)	44 (39.6)	111	

*Fisher exact test

HRCT Chest findings

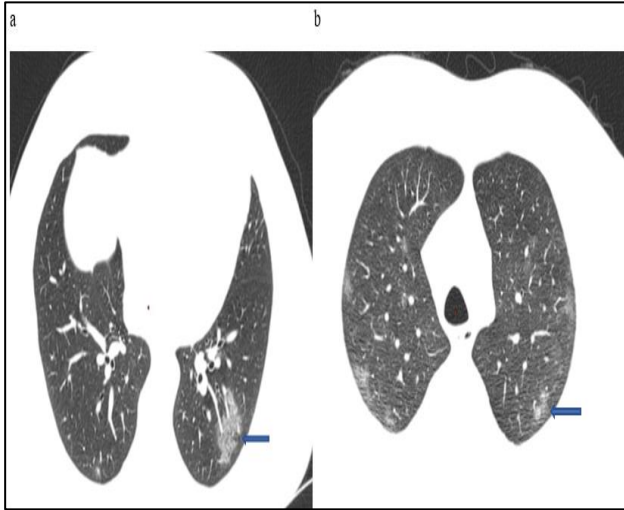


Figure 1 (a, b): HRCT axial sections show ground-glass opacities (blue arrow) in the peripheral distribution in bilateral lungs.

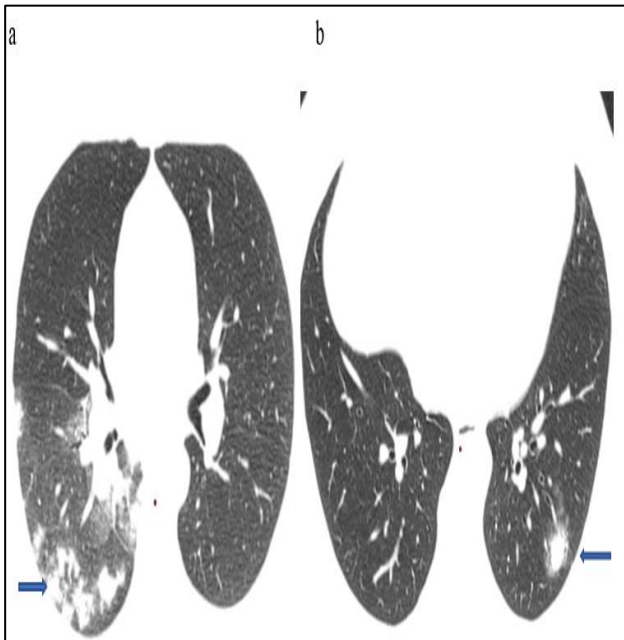


Figure 2 (a, b): HRCT lung axial sections show Air space opacifications (blue arrow) in the peripheral distribution in lower lobes.

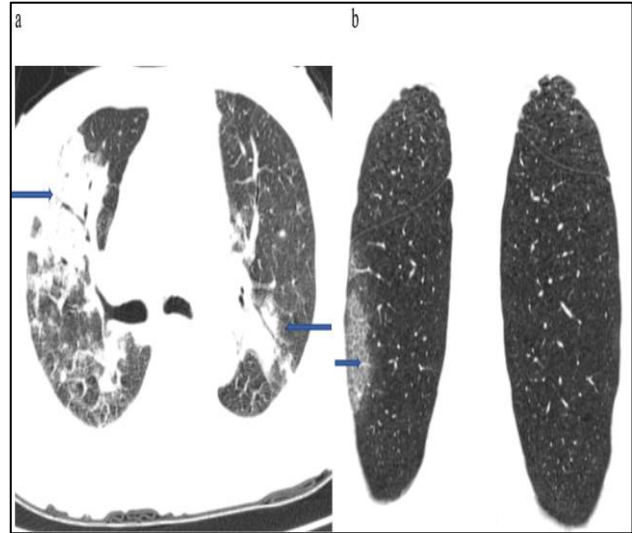


Figure 3: a) HRCT lung axial sections showing consolidation with air bronchogram (blue arrow) in right upper and lower lobes and left lower lobe in a covid patient; b) HRCT lung coronal section shows a crazy paving pattern (blue arrow) in the right lower lobe.

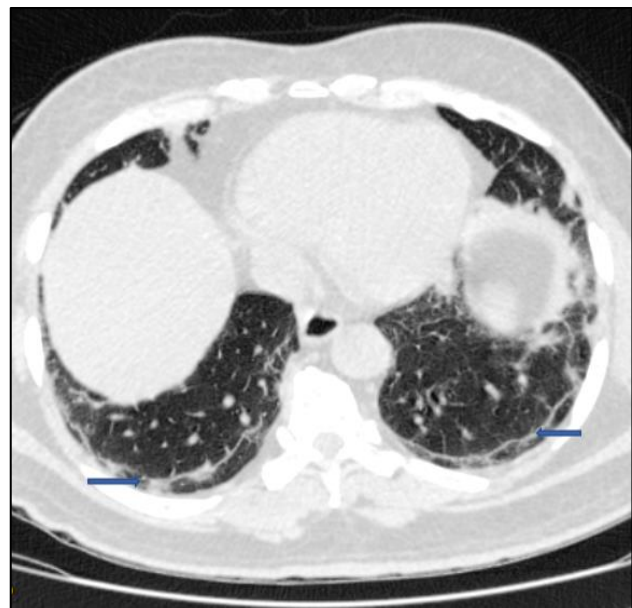


Figure 4: HRCT lung axial sections show subpleural linear bands (blue arrows) in bilateral lower lobes.

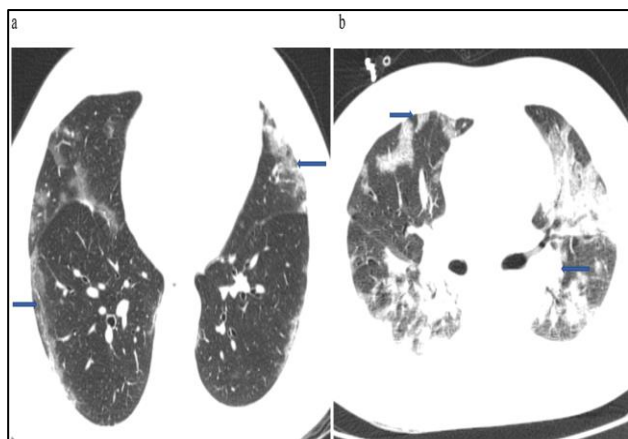


Figure 5: a) HRCT lung axial sections show peripheral distribution pattern (blue arrows) of predominant ground glass opacities bilaterally; b) HRCT lung axial sections show mixed distribution pattern (blue arrows) of opacities bilaterally in central and peripheral lung.

DISCUSSION

The lung lesions on the HRCT chest in RT-PCR-proven COVID-19 cases were characterised, quantified and correlated with the patient's clinical severity.

Primary lung lesions

Ground-glass haziness (GGH), air space opacifications (ASO), and consolidation with air bronchogram (CON) were the most common lesions observed in HRCT of Covid patients. Among these, ground-glass haziness (GGH) was the most common lesion seen in 84.6% of cohort patients. Most had bilateral multilobe lung involvement of ground glass haziness, and overall lesions were more common in the lower lobe segments. Airspace opacifications (ASO) with round morphology were the second most predominant lesion. Consolidation with air bronchogram (CON) was seen in a small number of patients. Few had normal CT without any lesions.

Predominant patterns in CT

Various patterns of lung findings were noted, ranging from predominant ground glass haziness pattern (52.2%), air space opacification pattern (24.3%), Mixed pattern (8.1%), consolidation with air bronchogram pattern (4.5%) to complete normal lung CT (10.8%). Our study found that ground glass haziness multifocal areas are the most common lung pattern. Most of our cases showed bilateral lung ground glass haziness and involvement of more than two lobes. The majority of the ground glass opacities showed peripheral distribution. Airspace opacifications with round morphology are the second most predominant pattern. Predominant peripheral distribution of airspace opacifications was noted. A mixed pattern without any predominant lesion pattern was seen in a few patients. Predominant consolidation

with air bronchogram pattern was the least common pattern observed. In this study, large consolidation with air bronchogram was more seen in the lower lobes and central distribution. A small number of patients had normal CT without any lesions.

The most common distribution pattern was a predominantly peripheral distribution of lung lesions (68.4%) followed by mixed distribution (16.2%) pattern of lesions, while others had a predominant central distribution (4.5%) pattern of lung lesions. The majority of patients in the study had bilateral lung involvement (93.9%), unilateral lung involvement was noted only in very few cases (6.1%), and all the unilateral lesions were ground-glass opacities.

Additional findings included subpleural linear bands (21.6%) and crazy-paving patterns (18.9%), followed by subpleural reticulations and fibrotic streaks (9.9%) and traction bronchiectasis (8.1%). Lung cyst/vacule within ground-glass opacities was seen in a few cases in CT (1.8%).

CT severity and clinical severity correlation

We noticed that there was an association between clinical severity and CT severity. We observed that there was a significant ($p < 0.001$) high positive correlation between CT severity and clinical severity ($r = 0.832$).

The majority of the cases had moderate (41.4%) or severe CT severity scores (39.6%), while some had mild (8.1%) and normal CT (10.8%). The clinical severity of most cases was moderate (57.6%), some were severe (21.6%), and a few were mild (10.8%) and critical (9.9%). The majority of cases with consolidation with air bronchogram (CON) showed severe CT scores and severe/critical clinical severity suggestive of advanced disease. Statistical tests performed to determine the association and correlation between CT severity and clinical severity showed a high positive correlation between CT severity and clinical severity with a statistically significant association of p value < 0.001 .¹⁹

There are some limitations of the study. This was a cross-sectional study conducted on each patient at a single time frame on the day of referral to the radiology department. Hence day of onset of clinical symptoms was not considered. Individual patient follow-up CT scans were not included.

CONCLUSION

Multifocal ground-glass opacities with peripheral distribution were the most characteristic HRCT lung finding observed in covid patients. This study shows that CT severity score is positively correlated with the clinical grading of the patient. CT severity score helps to stratify patients with COVID-19 pneumonia and predict clinical outcomes.

ACKNOWLEDGEMENTS

Authors are thankful to head of the department of radiology, all radiology faculty, radiology residents, CT technicians, clinicians at Sagar Hospitals, Tilak Nagar, Jayanagar, Bengaluru.

Funding: No funding sources

Conflict of interest: None declared

Ethical approval: The study was approved by the Institutional Ethics Committee

REFERENCES

1. Simpson S, Kay FU, Abbara S, Bhalla S, Chung JH, Chung M, et al. Radiological Society of North America Expert Consensus Statement on Reporting Chest CT Findings Related to COVID-19. Endorsed by the Society of Thoracic Radiology, the American College of Radiology, and RSNA- Secondary Publication. *J Thorac Imag.* 2020;35(4):219-27.
2. Zhou S, Wang Y, Zhu T, Xia L. CT features of coronavirus disease 2019 (COVID-19) pneumonia in 62 patients in Wuhan, China. *Am J Roentgenol.* 2020;214(6):1287-94.
3. Hefeda MM. CT chest findings in patients infected with COVID-19: review of literature. *Egypt J Radiol Nucl Med.* 2020;51(1):239.
4. Parekh M, Donuru A, Balasubramanya R, Kapur S. Review of the chest CT differential diagnosis of ground-glass opacities in the COVID era. *Radiology.* 2020;297(3):E289-302.
5. Chung M, Bernheim A, Mei X, Zhang N, Huang M, Zeng X, et al. CT imaging features of 2019 novel coronavirus (2019-nCoV). *Radiology.* 2020;295(1):202-7.
6. Dai H, Zhang X, Xia J, Zhang T, Shang Y, Huang R, et al. High-resolution chest CT features and clinical characteristics of patients infected with COVID-19 in Jiangsu, China. *Int J Infect Dis.* 2020;95:106-12.
7. Bernheim A, Mei X, Huang M, Yang Y, Fayad ZA, Zhang N, et al. Chest CT findings in coronavirus disease-19 (COVID-19): relationship to duration of infection. *Radiology.* 2020;295(3):200463.
8. Li K, Wu J, Wu F, Guo D, Chen L, Fang Z, et al. The clinical and chest ct features associated with severe and critical COVID-19 pneumonia. *Invest Radiol.* 2020.
9. Salaffi F, Carotti M, Tardella M, Borgheresi A, Agostini A, Minorati D, et al. The role of a chest computed tomography severity score in coronavirus disease 2019 pneumonia. *Medicine.* 2020;99(42):e22433.
10. Islam MN, Dipi RM, Mostafa SN, Datta A. Progression of disease in COVID-19 patients evaluated by chest CT imaging and correlated with clinical parameters. *Mymensingh Med J.* 2021;30(1):182-8.
11. Zhang J, Wang M, Zhao M, Guo S, Xu Y, Ye J, et al. The clinical characteristics and prognosis factors of mild-moderate patients with COVID-19 in a mobile cabin hospital: a retrospective, single-center study. *Front Public Health.* 2020;8:264.
12. Clinical Spectrum. COVID-19 Treatment Guidelines. Available from: <https://www.covid19treatmentguidelines.nih.gov/overview/clinical-spectrum/>. Accessed on 13 September 2021.
13. Martínez Chamorro E, Díez Tascón A, Ibáñez Sanz L, Ossaba Vélez S, Borrueal Nacenta S. Radiologic diagnosis of patients with COVID-19. *Radiología.* 2021;63(1):56-73.
14. Kayhan S, Kocakoç E. Pulmonary fibrosis due to COVID-19 Pneumonia. *Korean J Radiol.* 2020;21(11):1273-5.
15. José RJ, Manuel A, Gibson-Bailey K, Lee L. Post-COVID-19 bronchiectasis: a potential epidemic within a pandemic. *Expert Rev Respir Med.* 2020;14(12):1183-4.
16. Wasilewski PG, Mruk B, Mazur S, Póltorak-Szymczak G, Sklinda K, Walecki J. COVID-19 severity scoring systems in radiological imaging- a review. *Pol J Radiol.* 2020;85:e361-8.
17. Francone M, Iafrate F, Masci GM, Coco S, Cilia F, Manganaro L, et al. Chest CT score in COVID-19 patients: correlation with disease severity and short-term prognosis. *Eur Radiol.* 2020;30(12):6808-17.
18. Yang R, Li X, Liu H, Zhen Y, Zhang X, Xiong Q, et al. Chest CT severity score: an imaging tool for assessing severe COVID-19. *Radiol Cardiothorac Imag.* 2020;2(2):e200047.
19. Mukaka MM. Statistics corner: a guide to appropriate use of correlation coefficient in medical research. *Malawi Med J.* 2012;24(3):69-71.

Cite this article as: Jose J, Kalenahalli KV, Yerram S, Itagi RM, Eswara S. Pattern and distribution of lung parenchymal changes in COVID-19 infection on high resolution computed tomography: a descriptive cross-sectional study. *Int J Res Med Sci* 2023;11:223-9.